Deep Valley Radiation and Surface Energy Budget Microclimates. Part I: Radiation

C. DAVID WHITEMAN AND K. JERRY ALLWINE

Pacific Northwest Laboratory, Richland, Washington

LEO J. FRITSCHEN

University of Washington, Seattle, Washington

MONTIE M. ORGILL*

Pacific Northwest Laboratory, Richland, Washington

JAMES R. SIMPSON**

University of Washington, Seattle, Washington

(Manuscript received 25 March 1988, in final form 29 August 1988)

ABSTRACT

Solar and longwave radiation data are presented for five sites in Colorado's 650 m deep semiarid Brush Creek Valley (39°32'N, 108°24'W) during September 1984.

During the sunlit period of a nearly clear day, individual sites received 0.73–0.81 of the theoretical extraterrestrial solar radiation. Incoming solar radiation increased with elevation in the valley. Direct radiation made up 0.86–0.88 of the downward shortwave flux. On average, 0.12–0.21 of the incoming shortwave radiation was reflected at the individual sites. Strong variations in reflected solar radiation and outgoing longwave radiation occurred from site to site. Because of the large direct beam component, aspect and inclination angles of the valley surfaces had a strong effect on the solar radiation received. Contrasts between a southwest- and northeast-facing sidewall were significant. Shading from surrounding topography produced inter-site differences in both instantaneous and daily total radiation. Inter-site differences in most daily totals on a clear day were larger than standard deviations of the daily totals at a valley floor site computed over a 16-day period of variable weather. The ridgetop site, on account of its unobstructed view of the sky, had a higher average positive net radiation during the day and a higher average negative net radiation during the night than the valley stations.

Observations averaged over a 15-day period of variable weather illustrated the general effect of cloudy weather in reducing contrasts in radiation climate among sites.

A simple theoretical correction for radiation measured on a horizontal surface provided a useful estimate of net and global radiation on the underlying sloping surface.

1. Introduction

In high altitude mountainous areas, a variety of microclimates are produced by the exposure of different facets of the terrain surface to long- (i.e., terrestrial or atmospheric) and shortwave (i.e., solar) radiation. The energy inputs and outputs at the surfaces are a function of the azimuth and inclination angles of the surfaces relative to the incoming solar beam, as well as the surface characteristics and the characteristics of the surrounding terrain. The differing microclimates have far-reaching effects on the types of plant and animal communities that colonize the slopes and, in terms of man's economic pursuits, affect such things as the suitability of the mountainous area for the production of crops or for the growth of forage for domestic animals. We often recognize the existence of these microclimates indirectly by recognizing the diversity of ecosystems that are supported within a complicated mountainous region or by noticing the differing rates of erosion or snow melt. Such effects are accentuated in high altitude, dry, interior continental regions where we may speak of "radiation" climates.

A number of previous investigators have presented radiation data collected in continental mountainous areas (see Miller 1981 or Oke 1978 for a review of recent literature). Most such studies have focused on data collected at one or two sites where measurements were assumed to be representative of a valley floor or ridgetop location. Recently, however, as part of the U.S. Department of Energy's Atmospheric Studies in

* Current affiliation: White Sands Missile Range, Las Cruces, New Mexico.

** Current affiliation: University of Arizona, Tucson, Arizona.

Corresponding author address: Dr. C. David Whiteman, Battelle Pacific Northwest Laboratory, P.O. Box 999, Richland, WA 99352.

Complex Terrain (ASCOT) program, five stations were used to directly measure the diversity of radiation and surface energy balance microclimates at multiple locations in a single valley during a period in September and October of 1984. This paper will compare radiation components at the five stations on the nearly clear day of 25 September. The mean radiation budget at the stations during the period from 15 through 30 September will also be discussed, as will special observations designed to compare radiation received on pairs of radiometers oriented horizontally and parallel to the underlying slope. An accompanying paper (Whiteman et al. 1989) summarizes surface energy budget measurements at the five stations.

2. Experimental design

a. The Brush Creek Valley and measurement sites

Brush Creek (Fig. 1) is a 25-km tributary of Roan Creek, 55-km north-northeast of Grand Junction, Colorado. The valley runs from northwest to southeast, is 650 m deep at its lower end, has sidewalls with slopes of 30°–40°, and has a valley floor that falls 14 m per km. A succession of short box canyons (especially on the valley's east side) are the only tributaries to Brush Creek. The valley was chosen for the experiments partly for its near-ideal shape: it is a near-linear valley having no major tributaries, uniform sidewall angles, a simple well-defined drainage area, and relatively flat or rolling mesa-type ridgetops.

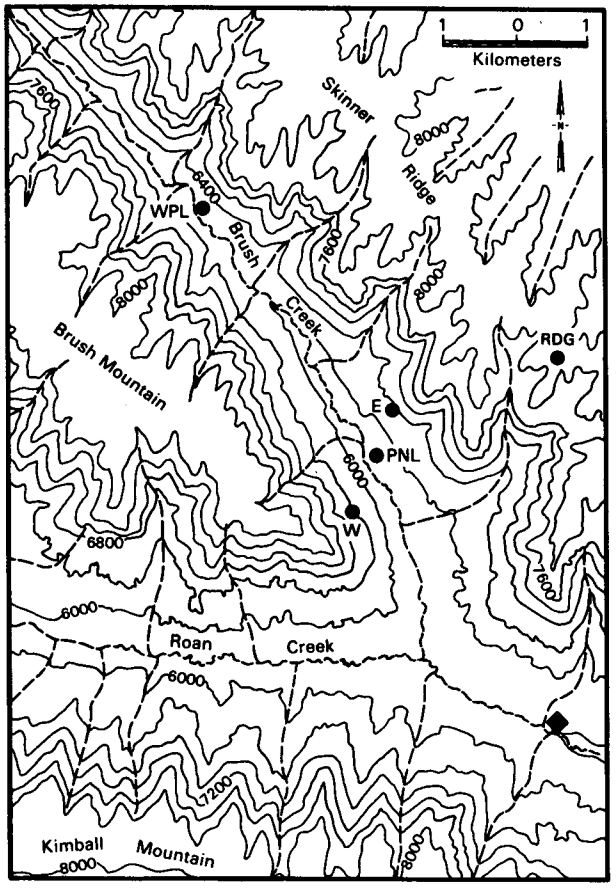

FIG. 1. Topographic map of the lowest 10 km of Colorado's Brush Creek Valley and its confluence with Roan Creek Valley. Elevations are in ft. Sites where the radiation stations were located are indicated by darkened circles. Stations W#1 and W#2 were located at the W site. The diamond indicates the Altenbern Ranch climate station.

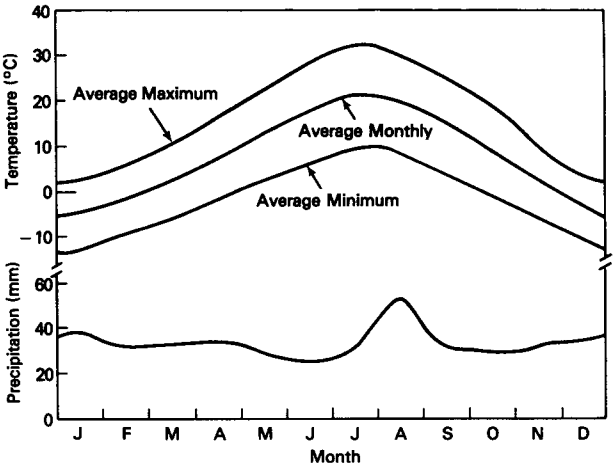

FIG. 2. Monthly mean temperatures and precipitation, 1947–1980, Altenbern Ranch, Colorado.

The Brush Creek Valley has a semiarid, continental climate. Monthly mean temperatures and precipitation at the Altenbern Ranch climate station near the mouth of Brush Creek (Fig. 1) are given in Fig. 2. Normal annual precipitation at this site (33-year period of record) is 394 mm (15.5 in.). Vegetation in the Brush Creek valley (Whiteman et al. 1987) varies significantly among the major valley surfaces, reflecting the increase of precipitation with elevation and the existence of different radiation microclimates on surfaces of different aspect and inclination.

The five radiation measurement sites (Fig. 1) were located on the valley's main topographic surfaces. Figure 3 presents photographs of each of the sites. Two sites, PNL and WPL, were located on the valley floor at different distances from the valley mouth. The PNL site was located in an area of natural sagebrush vegetation 2.8 km above the valley mouth. The WPL site was situated 7.2 km up the valley in an abandoned wheatgrass meadow on the valley floor, and will hereafter be called the meadow site. The meadow was surrounded by trees. A third site was situated on the broad ridgetop plateau (RDG) east of the valley. Another site was situated on the sparsely vegetated east (E) sidewall of the valley. The final site was located in a serviceberry thicket on the west (W) sidewall. Two stations (W#1 and W#2) were located side by side at this site for a time. The W#1 station collected data during the entire observational period with radiometers horizontal; the W#2 station was operated with radiometers parallel to the underlying slope after 26 September when the RDG site was decommissioned. Table 1 pro-

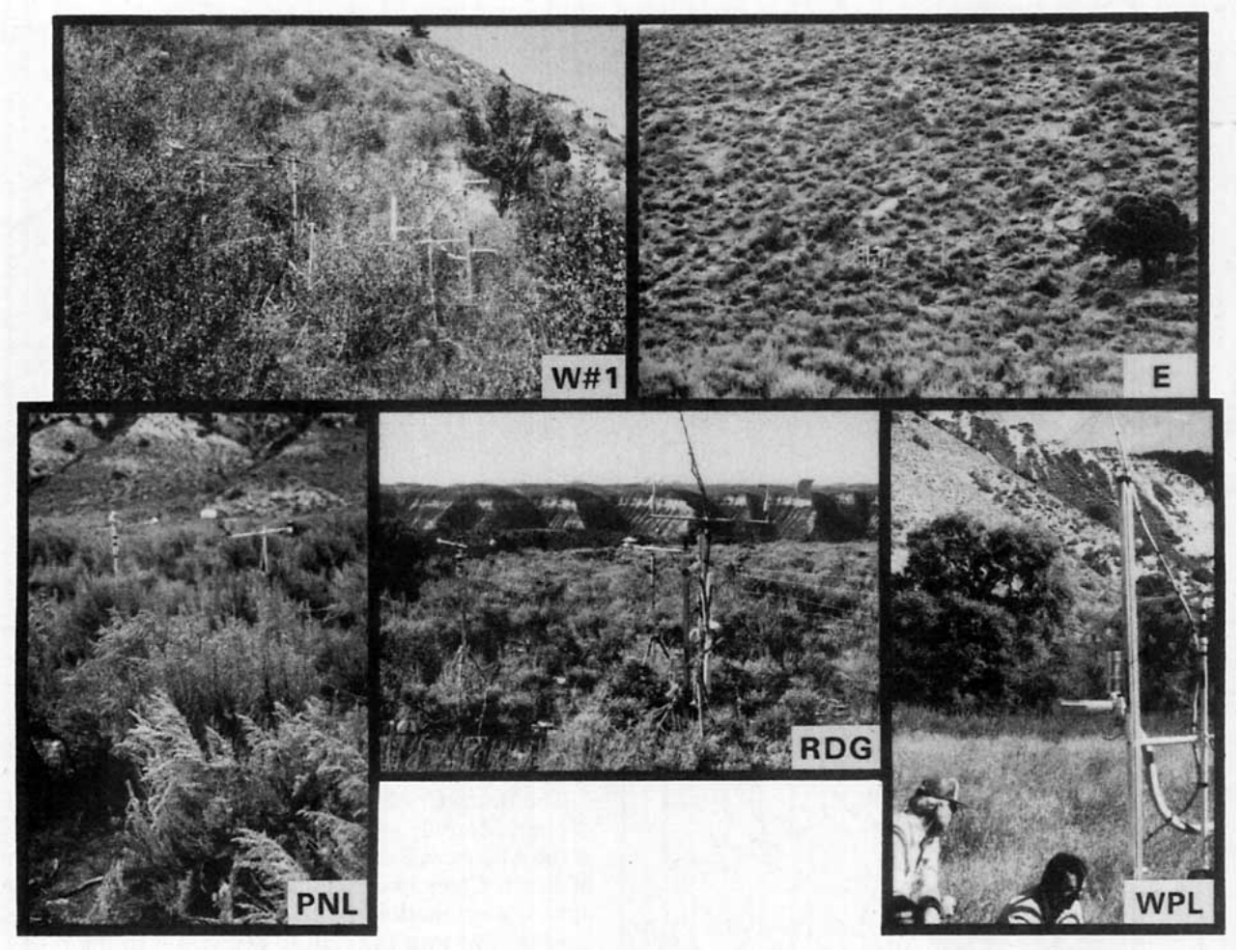

FIG. 3. Photographs of the experimental sites. W#1, from southeast; E, from southwest; PNL, from southwest; RDG, from east; WPL, from northwest.

vides further information on the site characteristics; Table 2 presents information on the vegetative cover at the five sites. The east and west sidewall sites were located on steep slopes. The other stations were located on level ground.

b. Equipment

An article by Fritschen and Simpson (1989) provides detailed information on the battery-powered data collection systems and instrumentation used at the Brush Creek stations. Pairs of Eppley Precision Spectral Pyranometers were used at the RDG, E and W sites to measure downward and upward shortwave radiation fluxes. Kipp and Zonen CM2 pyranometers were utilized at the WPL and PNL sites. Net radiation measurements were made with Fritschen miniature net radiometers. LiCor silicon cell pyranometers with shadow bands were used at all sites to measure diffuse radiation. Shadow band and spectral corrections were made as suggested by LiCor. Total hemispherical radiometers, as constructed from modified Fritschen net radiometers, were used at all sites to measure upward longwave radiation. The relative accuracies of the net and total hemispherical radiometers are 2% and 3%, respectively. The absolute accuracy is approximately 2% for the pyranometers, 10% for the net radiometers during daytime and 30% during nighttime.[1] Preexperiment

TABLE 1. Site characteristics.

Site	Latitude (dd mm ss)	Longitude (dd mm ss)	Altitude (m MSL)	Azimuth (deg true)	Slope (deg)
PNL	39 31 44	108 23 56	1795	—	—
RDG	39 32 27	108 22 11	2467	—	—
E	39 32 06	108 23 42	1935	240	42
W	39 31 22	108 24 07	1942	76	36
WPL	39 33 38	108 25 34	1857	—	—

[1] *Note Added in Proof:* These reported accuracies for the net radiometer were revised (lowered) in the galley proof stage on the basis of very recent, but preliminary, information that this widely used radiometer has a higher sensitivity to shortwave than to longwave radiation. The quantitative effects of this can not be accurately calculated until careful calibrations are performed, but the effects will be confined to the longwave radiation components and the net allwave radiation. A further communication will be made when information becomes available.

TABLE 2. Vegetation, height, and percent cover.

Site	Primary Type	Primary Height (m)	Primary Cover (%)	Secondary Type	Secondary Height (m)	Secondary Cover (%)
PNL	Sagebrush	0.80–1.50	30	Bunch Grass	0.20	5
RDG	Sagebrush	0.35–0.97	30	Oakbrush	2.25	10
E	Sagebrush	0.40–1.00	15	None	—	—
W	Bushes	1.50	40	Grass	0.40	10
WPL	Western Wheatgrass	0.25	70	Alfalfa	0.90	30

calibrations were performed on all radiation instruments. Data were collected using a data acquisition system controlled by a small personal computer, with data stored on audio cassette tapes.

c. *Collection and processing of data*

Data were collected continuously from 16 September through 6 October 1984. Unusually heavy precipitation occurred in early October, affecting the quality and quantity of data collected. Thus, this paper will focus on individual clear or nearly clear September days and data averaged over the September period of measurements. During the September measurement period, temperatures were near-normal and precipitation was somewhat higher than normal. Precipitation recorded at the Altenbern climate station was 12 mm on the 16th, 1 mm on the 21st, 8 mm on the 22nd, and 1 mm on the 24th of September.

Data from the radiation stations were sampled at 30-s intervals for the last 4 min of each 6-min period, with the resulting average labeled with the ending time of the 6-min period. Synchronization of the data collection systems and use of 6-min average data suggest that reported times will be accurate within about 6 min.

Radiation directed away from the surface was considered negative and radiation directed toward the surface was considered positive. Following this sign convention, the surface net all-wave radiation is given as the sum of net shortwave and net longwave radiation:

$$Q^* = K^* + L^*. \quad (1)$$

Net shortwave radiation is the sum of incoming and reflected shortwave radiation, $K^* = K\downarrow + K\uparrow$; net longwave radiation is the sum of incoming and outgoing longwave radiation, $L^* = L\downarrow + L\uparrow$; and incoming shortwave radiation is the sum of direct and diffuse radiation, $K\downarrow = S + D$.

The radiation balance is thus expressed as

$$Q^* = S + D + K\uparrow + L\downarrow + L\uparrow. \quad (2)$$

Direct measurements were made of each variable in the radiation balance equation except for S, determined as $K\downarrow - D$, and $L\downarrow$, determined as a residual.

5. Radiation budget for 25 September 1984

On 25 September 1984, the weather was nearly clear, although a few cirrus clouds were present in the early morning hours, and a layer of cirrostratus clouds made several advances into the valley from the south in the mid- to late afternoon. Radiometers at all stations were oriented horizontally on this date.

Figures 4 and 5 show radiation data measured on horizontal radiometers as a function of time for the Brush Creek sites on the 25th. Radiation data for the ridgetop and valley floor sites are shown in Fig. 4; data for the east and west sidewall sites are presented in Fig. 5.

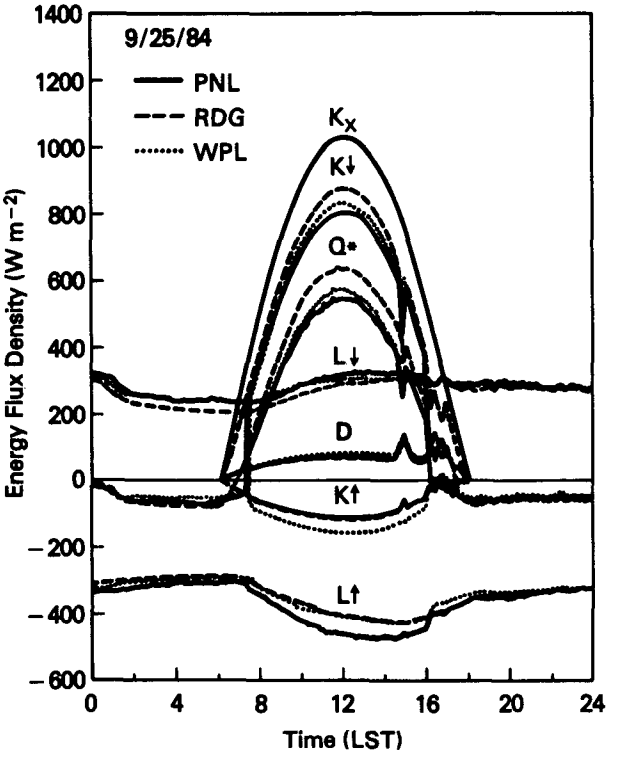

FIG. 4. 25 September 1984, radiation data from Colorado's Brush Creek Valley at sites PNL, RDG, and WPL. K_x is extraterrestrial solar radiation, $K\downarrow$ is incoming solar radiation, Q^* is net all-wave radiation, $L\downarrow$ is incoming longwave radiation, D is diffuse radiation, $K\uparrow$ is reflected solar radiation, $L\uparrow$ is outgoing longwave radiation.

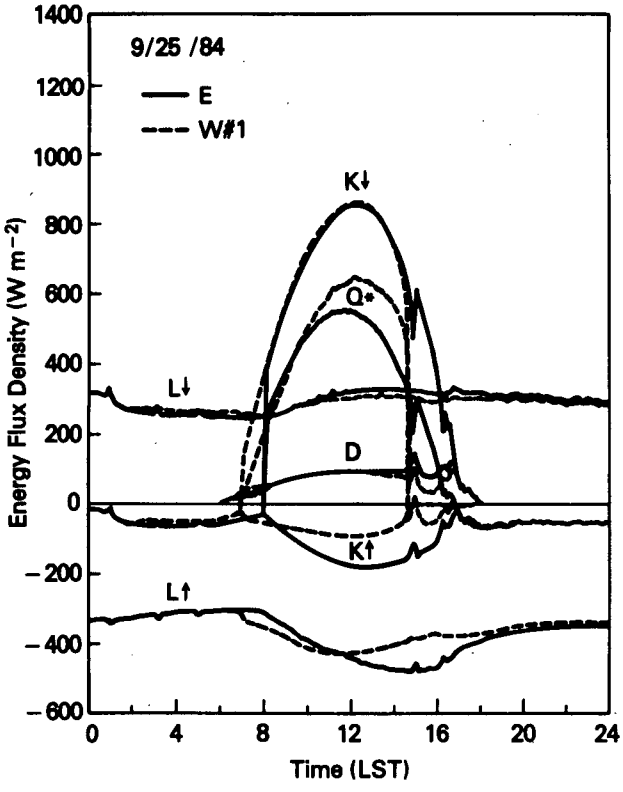

FIG. 5. 25 September 1984, measured radiation data from Colorado's Brush Creek Valley at the east and west sidewall sites. Measurements made on horizontal radiometers.

The direct solar and net radiation data from the horizontal radiometers at the east and west sidewall sites were translated to the underlying inclined sidewall surfaces. The results of this translation, which is described in section 6, are shown in Fig. 6. Subsequent discussion of radiation values at the east and west sidewall stations will refer to this translated data.

Time integration of the curves in Figs. 4, 5 and 6 provides daily and local sunrise to local sunset radiation totals listed in Table 3. Table 4 provides ratios of selected totals to characterize radiation microclimates. Individual components of the radiation budgets at the five stations will be summarized in the following paragraphs.

a. Extraterrestrial solar radiation and sunrise/sunset times

The 25th is a date quite near the autumnal equinox, when the sun rises due east, sets due west and the daylight period is 12 h. Extraterrestrial radiation, the solar radiation received outside the earth's atmosphere at the latitude and date in question, was calculated with a solar radiation model (Whiteman and Allwine 1986) and is provided in Fig. 4 for a horizontal surface and in Fig. 6 for unobstructed inclined plane surfaces parallel to the Brush Creek sidewalls. Astronomical sunrise (SR) and sunset (SS) on 25 September were at 0608 and 1803 LST and the sun climbed to an elevation angle of 49.8° at solar noon. The extraterrestrial solar flux curves provide useful benchmarks against which to assess the actual solar radiation received at the earth's surface. Since they are calculated for unobstructed plane surfaces (considering only self-shading of the surface), comparison with actual data allows an assessment of the effects of shading from the terrain surrounding a given site.

Astronomical sunrise and sunset (Fig. 4) marked the beginning and end of diffuse radiation receipt at all sites. Local sunrise (LSR) times at the individual sites are delayed relative to the theoretical curves at all sites except the ridgetop site, with the delay being nearly 2 h at the east sidewall site (Figs. 4 and 6). Local sunset (LSS) times are advanced from astronomical calculations at all sites, with advances ranging from 15 min at the ridgetop site to nearly 3.5 h at the west sidewall site. The result of the late sunrises and early sunsets is to substantially reduce insolation at the valley sites. Small amounts of diffuse radiation are received at all sites between astronomical and local sunrise and between local and astronomical sunset, but the delay in receiving the much larger direct radiation component is critical to the daily radiation totals. For example, at the east sidewall site (Table 3) daily total extraterrestrial radiation is 32.47 MJ m^{-2} for a theoretical unobstructed horizontal surface, but is 28.99 MJ m^{-2} on

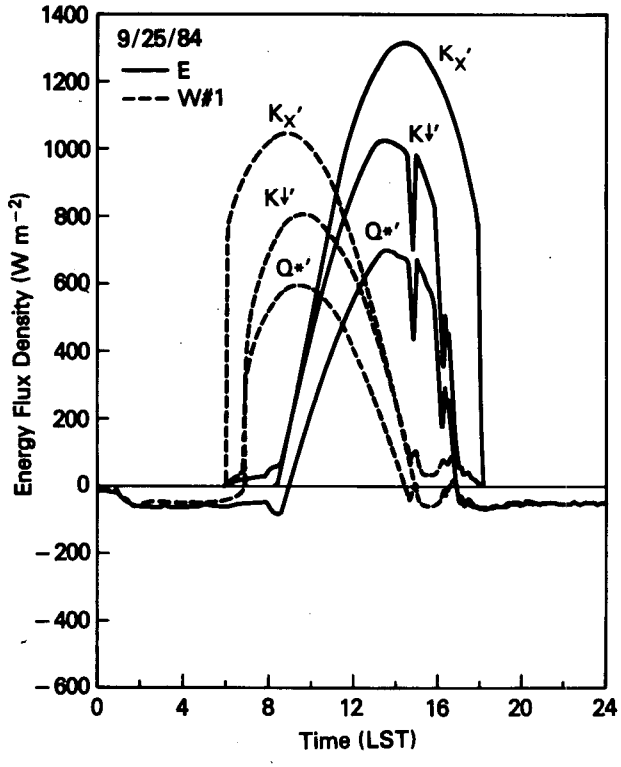

FIG. 6. Theoretical calculations of extraterrestrial, global and net radiation on the inclined surfaces of the east and west sidewall sites.

TABLE 3. Radiation totals* calculated from 6-min averages, 25 September 1984.

Site	Time (LST)	K'_x	$K\downarrow'$	$K\downarrow$	S'	D	$K\uparrow$	$K^{*\prime}$	$L\downarrow$	$L\uparrow$	L^*	$Q^{*\prime}$	Q^*	N
						Daily totals (MJ m^{-2})								
PNL	0000–2400	28.18	19.92	19.92	17.39	2.53	−2.89	17.03	24.44	−32.03	−7.59	9.45	9.45	240
RDG	0000–2400	28.18	22.68	22.68	19.99	2.69	−3.20	19.48	22.54	−29.91	−7.37	12.11	12.11	240
E	0000–2400	32.47	21.25	20.58	18.29	2.96	−4.26	16.99	25.07	−32.33	−7.26	9.73	9.06	240
W#1	0000–2400	24.03	17.18	18.52	14.53	2.65	−2.14	15.04	24.58	−31.11	−6.53	8.51	9.85	240
WPL	0000–2400	28.18	20.53	20.53	17.81	2.72	−4.12	16.41	23.89	−29.85	−5.96	10.45	10.45	240
						LSR–LSS** Totals (MJ m^{-2})								
PNL	0724–1606	25.87	19.43	19.43	17.31	2.12	−2.85	16.58	9.49	−13.86	−4.37	12.21	12.21	89
RDG	0612–1748	28.17	22.68	22.68	19.99	2.69	−3.20	19.48	11.40	−16.07	−4.67	14.81	14.81	118
E	0806–1654	28.99	21.03	20.33	18.29	2.74	−4.22	16.82	9.84	−13.98	−4.14	12.68	11.98	90
W#1	0700–1436	21.61	16.55	17.88	14.52	2.03	−2.08	14.47	7.92	−11.21	−3.29	11.19	12.52	78
WPL	0736–1606	25.62	20.01	20.01	17.69	2.32	−4.05	15.96	9.02	−12.27	−3.25	12.71	12.71	87

* Primed quantities indicate slope-parallel radiation totals; other quantities are measurements made on horizontal radiometers. PNL, RDG and WPL sites are horizontal sites; E and W#1 sites have inclination angles of 42 and 36°, respectively. N is the number of 6-min averages in the total period.

** LSR–LSS—local sunrise to local sunset.

the same surface when integrated between the actual times of local sunrise and local sunset.

b. *Incoming solar radiation*

Incoming solar radiation is the sum of a directional, or direct beam, component and a diffuse component. The diffuse component comes predominantly from the sky, but in mountainous areas may include reflections from terrain within the radiometer's viewing hemisphere.

Receipt of diffuse radiation begins near astronomical sunrise and persists until astronomical sunset. It is the sole shortwave component received at a deep valley site before local sunrise and after local sunset. During the daytime period (LSR–LSS) the relative fractions of diffuse and direct radiation are dependent on the turbidity of the atmosphere. The more turbid the atmosphere and the longer the atmospheric path length, the larger the fraction of diffuse radiation scattered out of the solar beam. In Fig. 4, for example, diffuse radiation at the horizontal sites varies smoothly from SR to SS, attaining peak values of generally less than 90 W m^{-2} at solar noon. During cloudy periods, loss of the direct component is only partly compensated by an increase in the diffuse component, resulting in a net decrease in incoming solar radiation. On clear days at sea level, typically about 0.15–0.20 of the daily total incoming solar radiation is in the diffuse component (Miller 1981). In the high altitude Brush Creek Valley (Table 4), diffuse radiation makes up only 0.11–0.13 of the total. This figure would be slightly lower on a completely clear day. Instantaneous values of diffuse radiation (Figs. 4 and 5) do not vary greatly from site to site. During noncloudy daytime periods diffuse radiation generally differed by less than 25 W m^{-2} among the sites. Daily totals of diffuse radiation varied from 2.53 to 2.96 MJ m^{-2} at individual sites (Table 3).

TABLE 4. Ratios of radiation totals from Table 3, 25 September 1984.

Site	$\frac{\lvert K\uparrow\rvert}{K\downarrow}$	$\frac{K\downarrow'}{K'_x}$	$\frac{Q^{*\prime}}{K'_x}$	$\frac{D}{K\downarrow}$
		Daily ratios		
PNL	0.15	0.71	0.34	0.13
RDG	0.14	0.80	0.43	0.12
E	0.21	0.65	0.30	0.14
W#1	0.12	0.71	0.35	0.14
WPL	0.20	0.73	0.37	0.13
		LSR–LSS ratios		
PNL	0.15	0.75	0.47	0.11
RDG	0.14	0.81	0.53	0.12
E	0.21	0.73	0.44	0.13
W#1	0.12	0.77	0.52	0.11
WPL	0.20	0.78	0.50	0.12

Diffuse radiation is generally nonisotropic, coming unequally from different parts of the sky (e.g., see Steven and Unsworth 1979). Different orientations to the vertical of a diffuse radiometer will therefore affect the measured values. At deep valley sites, changes in radiometer orientation affect the view of surrounding topography, thus affecting receipt of reflected radiation. Measurements of this effect at a single site will be presented in section 6.

Direct radiation plays a key role in forming the microclimates in the valley because the incoming solar radiation is strong and the diffuse component is relatively weak. Incoming solar radiation is a high fraction of the extraterrestrial (Table 4) in the high elevation

valley. Specifically, during the LSR to LSS period, downward solar radiation is 0.73 to 0.81 of the extraterrestrial; the solar beam loses only 0.19 to 0.27 of its energy content in passing through the earth's atmosphere. This loss is less than normally experienced at low altitude sites. For example, according to Oke (1978), Davis et al. (1970) report a loss of 0.36 during a clear day in late August at Grimsby, Ontario. The high fraction of energy in the direct component produces characteristics typical of "radiation" microclimates. Incoming solar radiation in such microclimates is predominantly a vector quantity, and strong climatic contrasts are generated on surfaces that differ in azimuth and inclination relative to the solar beam. Variation in the receipt of direct radiation is also the primary cause of variations in other radiation components. Thus, the inclined sidewall sites (Fig. 6) have markedly different diurnal courses of radiation. The "west" sidewall, facing northeast, experiences high downward solar fluxes immediately after the slope is illuminated, and peak insolation (nearly 800 W m^{-2}) occurs before 1000 LST. Fluxes are weak in the afternoon and the sun sets on the slope by 1436 LST. In contrast, the "east" sidewall, facing southwest, has weak insolation in the morning but attains a strong peak of over 1000 W m^{-2} in the early afternoon. Vegetation on the east and west sidewalls is consistent with these contrasting radiation climates. Little vegetation grows on the dry, intensely heated southwest-facing sidewall, while the more moist northeast-facing sidewall supports a dense cover of serviceberry and mountain mahogany bushes.

As the shadow from the ridge west of the valley moves up the east sidewall in the afternoon, there is a very strong contrast within an along-slope distance of tens of meters between sites that are shaded and sites that are still receiving large solar radiation fluxes. This characteristic is typical of radiation microclimates.

Instantaneous global radiation increases with elevation in the valley (Figs. 4 and 5), illustrating the effects of atmospheric absorption and back-scattering of the solar beam. Daily and LSR–LSS incoming solar radiation totals (Table 3) are highest at the ridgetop site which, because of its longer daylight period, receives larger totals than the other horizontal sites (WPL and PNL). Totals at the east sidewall site rival those received at the ridgetop site, despite the much shorter sidewall daylight period, because of favorable orientation of the sidewall relative to the solar beam. Other slopes would be even more favorably oriented. For example, theoretical calculations show that unobstructed south-facing slopes of 30°–50° would receive about 35% more radiation than the ridgetop site.

c. *Reflected solar radiation*

The amount of incident solar radiation reflected at a site depends on the reflectance of vegetation and bare soil at that site. For nonisotropic reflectors, reflection will be a function of the incident angle of the solar beam. Figures 4 and 5 show reflected radiation as a function of time, as measured on horizontal downward-looking radiometers. Reflected radiation at the level sites is symmetric about solar noon with nearly identical values at the PNL and ridgetop sites. The grass-covered WPL site had higher reflected radiation, attaining midday values of 150 W m^{-2}. The sidewall sites, on the other hand, had distinctly asymmetric reflected radiation curves. Interpretation of these curves is complicated by the fact that radiometers were oriented horizontally while located above sloping surfaces.

Figure 7 shows the variation with time of albedo at the five sites, where albedo is defined as the absolute value of $K\uparrow/K\downarrow$, i.e., radiation values are uncorrected measurements on horizontal radiometers. Some interesting variations of albedos with time are apparent in the figure. At the nonsidewall sites, albedos are relatively invariant in midday, but are elevated significantly in the morning. These sites were on relatively flat ground, but slope angles were not measured. A possible explanation for the elevated morning albedos is related to the horizontal orientation of the downward-looking pyranometer and its receipt of reflected radiation when reflection at the underlying surface is partly specular. These slightly inclined surfaces would have a southwest aspect. Another possible explanation is instrumental error due to reflections inside the radiometer domes. This effect has been reported for low incidence angles over vegetated surfaces by Brown et al. (1970).

Albedos at the sidewall sites are especially interesting. The east sidewall has a steady albedo increase during daytime, which could be explained again by the receipt of specularly reflected radiation on the horizontal radiometer. The west sidewall site had a period of steady albedos in midday, elevated albedos in morning, and decreased albedos in afternoon. The midday invariance is probably caused by nearly isotropic reflection from

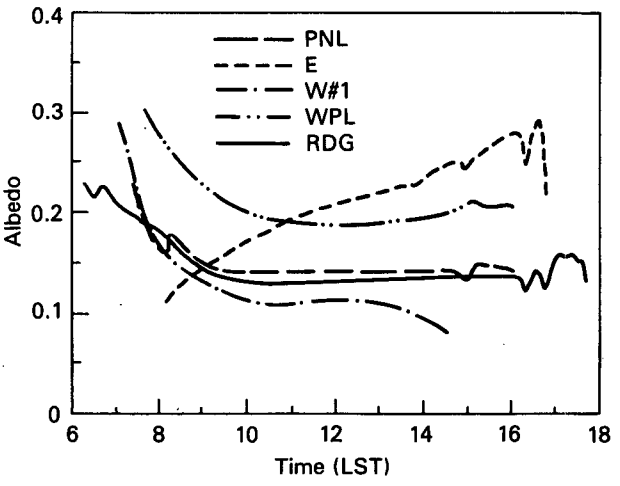

FIG. 7. Albedos, 25 September 1984.

bushes when solar incidence angles are high; the enhanced albedos in morning and decreased albedos in afternoon are again an indication of increased specular reflection with low solar incidence angles where we must consider again the orientation of the pyranometer. At midday the highest reflectance (0.22) occurred at the bare east sidewall site. The grassy meadow site also had relatively high reflectances (0.18). The PNL and ridgetop sites had similar vegetation and similar albedos (0.14 and 0.13, respectively), while the albedo of the brushy west sidewall site was only 0.11. The daily and LSR–LSS average albedos for the sites (Table 4) differed little from the midday values.

d. Net solar radiation

Net solar radiation is the sum of incoming and reflected solar radiation. Since reflected radiation is only 0.14–0.21 of the incoming radiation, net solar radiation has the approximate shape of the incoming solar radiation curves and is the largest of the net radiation components (i.e., compared to net longwave and net all-wave radiation), attaining LSR–LSS totals of 14.47 to 19.48 MJ m^{-2}.

e. Downward longwave radiation

Downward longwave radiation is the largest supplier of energy to valley ecosystems over the 24 h period (Table 3). Unlike the solar radiative components, the longwave components are reasonably steady night and day, and provide a moderating influence on ecosystems. In deep valleys, this radiation stream comes from two sources—longwave radiation from the atmosphere and longwave radiation from the surrounding terrain. The fraction of energy coming in these various components depends, in part, on the relative fractions of sky and ground seen in the viewing hemisphere of the surface; it also depends on the atmosphere's transmittance to longwave radiation, which depends on the concentrations of radiatively important atmospheric constituents. In the case of the Brush Creek sites, sky view factors (sky fraction of hemisphere) were: PNL, 0.74; RDG, 0.92; E, 0.72; W#1, 0.74; and WPL, 0.67. With time (Figs. 4 and 5), this radiative component undergoes a steady long-term decrease from mid afternoon through the night. After sunrise, as the atmosphere and ground surfaces warm, downward longwave radiation recovers from its nighttime minimum.

Of the major radiative components, downward longwave radiation has the smallest variation from site to site. This variation among sites is on the order of 40 W m^{-2}, day and night. The variation among sites can be considered in terms of the effective radiating temperature of the viewing hemisphere with the use of the Stefan–Boltzmann law (Fig. 8), assuming an atmospheric emittance of 1. With the low humidities in this climate setting, the ridgetop site views a cold radiating sky day and night and views very little of the surrounding, relatively warmer, terrain. Effective radiating temperatures drop to −27°C at sunrise. During nighttime, the east and west sidewall sites see relatively warm temperatures on account of their favorable positions relative to the valley temperature inversion and on account of their larger view of the warm valley sidewalls. The valley floor sites receive longwave radiation intermediate in magnitude between the ridgetop and sidewalls sites.

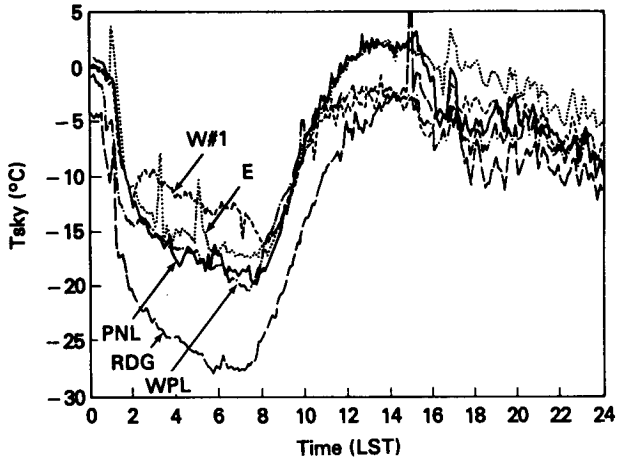

FIG. 8. Effective sky radiating temperatures at the five Brush Creek sites, 25 September 1984.

f. Upward longwave radiation

Longwave radiation emitted by ecosystems is the largest of all the daily averaged radiative fluxes (Table 3). During the daytime period this radiative loss from the ecosystem counters the large gains from incoming solar radiation, acting to dissipate excess heat that would otherwise be fatal to some plant and animal communities. During nighttime, on the other hand, longwave losses continue (although at slower rates as ecosystem temperatures drop) and can produce ecosystem stress. On 25 September, nighttime radiative losses aided in dropping ecosystem temperatures below the freezing level. This is seen in Fig. 9, where the upward radiative fluxes have been converted to effective radiating temperatures using the Stefan–Boltzmann law for an assumed emittance of 1. Effective radiating temperatures were generally lowest at the ridgetop and meadow sites. Diurnal oscillations in radiating temperature were smallest at the west sidewall site (24°C) and at the meadow and ridgetop sites (both 25°–30°C). Daytime radiating temperatures reached peak values of around 30°C at the valley floor site having natural sagebrush vegetation and at the east sidewall site.

The differential heating of the two sidewalls was clearly seen in the outgoing longwave radiation data (Fig. 9), with strong morning heating of the west sidewall ecosystems and afternoon heating of the east side-

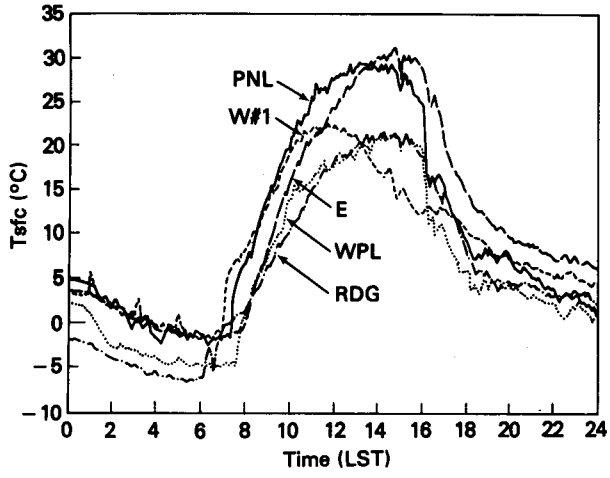

FIG. 9. Effective ground radiating temperatures at the five Brush Creek sites, 25 September 1984.

wall ecosystems. At all sites except the ridgetop site, radiating temperatures (Fig. 9) and the magnitude of upward longwave radiation (Figs. 4 and 5) rose and dropped suddenly at the times of local sunrise and sunset.

g. Net longwave radiation

Outgoing longwave radiation is partly counterbalanced by incoming longwave radiation so that net longwave radiation (Table 3) is much smaller than net solar radiation.

h. Net all-wave radiation

Net all-wave radiation is equivalent to net longwave radiation at night and is dominated by net shortwave radiation during the day. Net all-wave radiation totals during daytime are about 50% of incoming extraterrestrial radiation totals (Table 4). During daytime (Figs. 4 and 5) the course of the net radiation curve at a given site is defined primarily by the receipt of direct radiation. The dry continental atmosphere over the Rocky Mountains produces relatively meager amounts of downward longwave radiation so that the net longwave loss decreases net all-wave radiation substantially during the day. Daytime net all-wave radiation totals range from 0.76 (W#1) to 0.86 (E and WPL) of the ridgetop value. Site to site differences are primarily related to receipt of direct radiation and thus depend on the length of the daytime period and the orientation of the slope.

Nighttime net radiative loss totals (LSS-LSR) at the various sites were 1.02, 1.09, 0.99, and 0.84 of the losses at the ridgetop site for the PNL, E, W#1, and WPL sites, respectively. Dividing the total losses by the lengths of the nighttime periods at the individual sites results in average rates of energy loss that are 0.84, 0.90, 0.75, and 0.67 of the ridgetop loss rates. Thus, the largest rate of nighttime energy loss occurs at the ridgetop site where longwave fluxes from the cold sky are particularly small.

Large rates of nighttime loss and large daytime gains at the ridgetop site support the concept of elevated terrain areas being sources of heating during day and cooling during night. This concept has been used to explain the development of mountain-plain wind circulations and, in the case of ridgetops, the development of along-slope wind circulations.

The fact that net all-wave radiation is a large positive value during the day and a small negative value during the night points out the general lack of a radiative balance at a given instant in time, or diurnally. Deficits or excesses in the radiation budget must be made up through fluxes of energy from nonradiative sources. The means by which the Brush Creek Valley radiative imbalances are overcome by soil, sensible and latent heat fluxes is discussed in the companion paper by Whiteman et al. (1989).

6. Horizontal versus slope-parallel exposure of sensors

Apart from considerations of the performance of inclined radiometers, several operational considerations come into play when exposing radiometers over inclined surfaces. Where the emphasis of the research is on interstation comparisons it is sometimes preferable to expose all radiometers horizontally, whether installed over horizontal or inclined surfaces. This has operational advantages, especially with respect to directed radiation streams, since the field technician can easily compare the timing and magnitude of the radiation at different sites and verify that equipment is performing as expected. This also obviates the necessity of determining the azimuth and inclination angles of the underlying slope, which can be quite subjective because it involves an implied slope length scale. Nonetheless, when one wishes to measure the radiation income per unit area of the sloping surface, a direct measurement is preferable. Conversion from horizontal measurements is nontrivial because the hemisphere viewed by the horizontal and slope-parallel radiometers may include quite different portions of the sky and surrounding terrain. The measurements will be affected by the distribution of sky radiation as well as the differing reflections or emissions from viewed terrain surfaces.

An exact means exists for calculating direct beam radiation on unobstructed horizontal and inclined surfaces, using the equations

$$S = S_{\perp} \cos Z, \quad \text{and} \tag{3}$$

$$S' = S_{\perp} \cos\beta, \tag{4}$$

where $S_{\perp}$ is the solar radiation falling on a surface perpendicular to the solar beam, Z is the solar zenith angle, and β is the angle between the solar beam and the normal to the slope. The cosines of the angles are given as

$$\cos Z = \sin\phi \sin\delta + \cos\phi \cos\delta \cos h, \quad \text{and} \quad (5)$$

$$\cos\beta = [\sin\phi \cos h(-\cos a \sin i) - \sin h(\sin a \sin i) + (\cos\phi \cos h) \cos i] \cos\delta + [\cos\phi(\cos a \sin i) + \sin\phi \cos i] \sin\delta, \quad (6)$$

where ϕ is latitude, δ is solar declination, h is hour angle, a is the azimuth angle of the horizontal projection of the normal to the inclined surface (clockwise from north), and i is the slope inclination angle.

The relationship between direct radiation on a horizontal surface and on an inclined surface is obtained by dividing (4) by (3) to obtain:

$$\frac{S'}{S} = \frac{\cos\beta}{\cos Z}. \quad (7)$$

This theoretical relationship is illustrated in Fig. 10 for the Brush Creek Valley on 29 September for a 30° sidewall inclination angle and for various slope aspect angles. Since diffuse and total radiation were measured with horizontal radiometers on the Brush Creek sidewalls, direct radiation on the horizontal surface is known from the equation $S = K\downarrow - D$, and incoming solar radiation can be estimated on the underlying sidewall surface by the equation

$$K\downarrow' = \frac{\cos\beta}{\cos Z}(K\downarrow - D) + D. \quad (8)$$

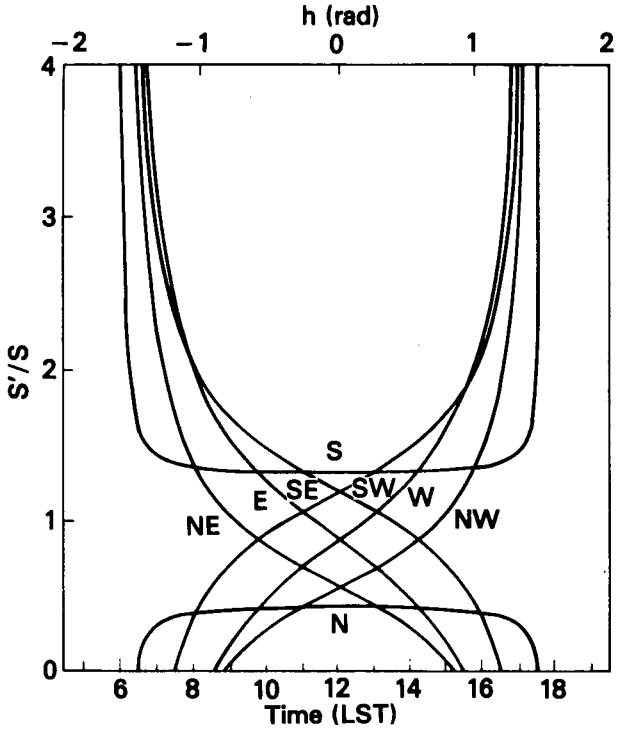

FIG. 10. Ratio of direct radiation on a 30° sloping surface of indicated aspect and direct radiation on a horizontal surface as a function of hour angle and local standard time. Calculations are made for 25 September at the latitude of the Brush Creek Valley.

This formula has been used to provide radiation estimates for the inclined east and west sidewall sites.

Transformation of other radiation budget terms is complicated by a number of factors. A special experiment was therefore designed to investigate directly the effects of radiometer exposure over slopes. For this purpose the ridgetop station was decommissioned on 26 September, reinstalled adjacent to the existing west sidewall station, and operated through 6 October 1984. The original station, termed W#1, had all radiometers installed horizontally. The new station, W#2, had identical equipment to the first station but was installed with radiometers parallel to the underlying slope. The azimuth and inclination angles of the underlying slope were estimated independently by two observers. Radiometers were then set to the averaged values listed in Table 1 with a compass and an inclinometer. Unfortunately, a poor electrical connection at the W#2 net radiometer caused loss of these data intermittently during the period of the experiments. Net radiation data were reconstructed at the W#2 site by calculation as a residual from (2), where net longwave radiation was substituted from the W#1 station. This was justified by the near-equality of net longwave radiation values at the two stations during periods when both net radiometers were operational. Measurements of radiation budget terms at the W#1 and W#2 sites are compared for the clear day of 29 September in Fig. 11.

The most striking differences in the curves involve the net all-wave and downward solar radiation terms. These terms have large direct radiation components and, as we have seen above, the effect of the slope and aspect angles of the receiving surface are quite significant on the temporal behavior and magnitude of the curves. Differences in other radiation budget terms were noted at the two stations. Upward longwave radiation was slightly stronger on the horizontal radiometer, especially during midday. The reasons for this are not entirely clear. Reflected shortwave radiation was slightly stronger on the inclined radiometer in the morning, but significantly higher on the horizontal radiometer in the afternoon. Diffuse radiation was enhanced on the inclined radiometer in the morning. This radiometer faces the sun more directly in the morning and the circumsolar diffuse radiation component apparently is responsible for this feature of the curve. The net radiation curve for the inclined surface shows a sudden drop just after sunset that is recovered only slowly over a period of 2 or 3 h. This appears to be an instrument malfunction and, since downward longwave radiation is calculated as a residual, the same feature appears in the latter curve as well.

Measurements on the horizontal and inclined radiometers, except for net all-wave and incoming solar radiation, differ less than 50 W m^{-2} during the entire day. This suggests a means of translating to inclined surfaces measurements of net all-wave radiation made on horizontal surfaces. Assuming that the sum of dif-

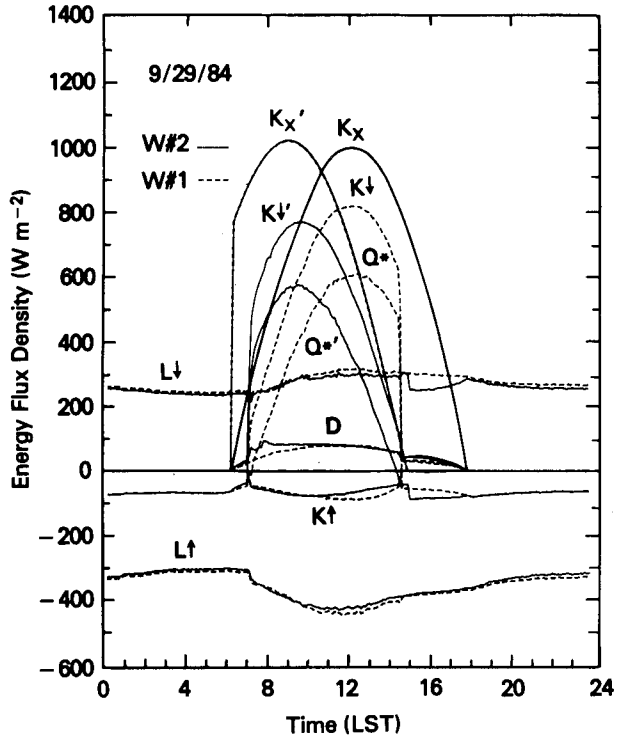

FIG. 11. Comparison between measurements made with horizontal radiometers (W#1) and measurements made with radiometers oriented parallel to the underlying 36° slope (W#2). West sidewall site, 29 September 1984.

fuse, reflected solar, downward longwave and upward longwave radiation does not differ significantly when measured on horizontal and slope-parallel sensors, the following formula can be used to estimate net all-wave radiation on an inclined surface:

$$Q^{*\prime} = (K\downarrow - D)\left(\frac{\cos\beta}{\cos Z} - 1\right) + Q^{*}. \qquad (9)$$

This formula has been used to estimate net all-wave radiation at the inclined east and west sidewall sites.

Figure 12 compares the measurements on inclined radiometers with the results of translating horizontal measurements using (8) and (9). The shapes and magnitudes of the curves compare well on clear days, except for an overestimate of translated values for an hour or two after local sunset. Further, the use of the two translation equations can be justified by considering that daily totals for 29 September calculated for the two curves in Fig. 12(a) differ by only 2.4%, and for Fig. 12(b) differ by 0.3%.

How closely will daily totals on horizontal radiometers approximate the true values on inclined surfaces for components other than net all-wave radiation and downward solar radiation? By integrating under the curves in Fig. 11, we find that horizontal totals are 2% higher than the true totals for upward longwave radiation, 16% lower for reflected solar radiation, and 13% higher for diffuse radiation. These last two percentage errors are appreciable, but represent relatively small amounts of radiation, considering the overall budget.

7. Radiation budget for 16–30 September

Data, to this point, have been selected to illustrate the radiation budget on a nearly clear day. The full period of observations, however, included variable weather that is more representative of the fall climate of the valley. Data will be presented in this section to illustrate longer term means and variabilities in daily radiation budgets. For this purpose the 15-day period from 16 through 30 September was chosen. This period had mean temperatures near climatic normals, but precipitation and, presumably, cloudiness were somewhat above normal. Table 5 presents the means of daily periods and local sunrise to local sunset periods for the PNL valley floor site for 15 days. This table can be compared to PNL values in Table 3 to see the effects of variable weather on the totals. Standard deviations and coefficients of variation are also presented in Table 5. The coefficient of variation, defined as the ratio of the standard deviation to the mean, is a measure of relative variation of the radiation parameters.

The primary effect of the variable weather is to mod-

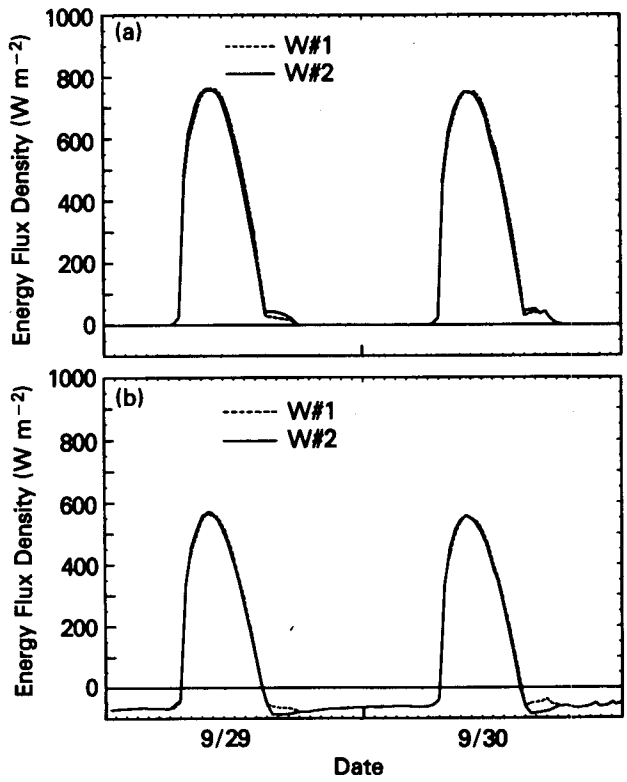

FIG. 12. Comparison between radiation measured on slope-parallel radiometers at the W#2 site, and radiation measured on horizontal radiometers at the W#1 site but translated to the sloping surface using (8) and (9). (a) downward solar radiation, and (b) net radiation.

TABLE 5. Daily average radiation totals and their standard deviations (MJ m^{-2}), as calculated for the PNL valley floor site over the period 16–30 September 1984. (s = standard deviation; μ = coefficient of variation)

Parameter	K_x	$K\downarrow$	D	$K\uparrow$	K^*	$L\downarrow$	$L\uparrow$	L^*	Q^*
Daily average	28.65	15.82	4.65	−2.26	13.56	28.57	−34.14	−5.58	7.99
s		3.40	1.94	0.50	2.90	2.58	1.80	1.38	2.07
μ		0.21	0.42	0.22	0.21	0.09	0.05	0.25	0.26
LSR–LSS average	26.19	15.41	4.33	−2.22	13.20	11.32	−14.41	−3.09	10.07
s		3.42	1.89	0.51	2.92	0.97	0.85	0.82	2.20
μ		0.22	0.44	0.23	0.22	0.09	0.06	0.27	0.22

erate the microclimate of the PNL site by decreasing direct radiation. Net longwave radiative loss is reduced in the climatological mean and the fraction of diffuse solar radiation is increased.

The 15-day period of interest is near the time of the autumnal equinox, when days are getting shorter and the flux on a horizontal surface at solar noon is steadily decreasing. Daily total extraterrestrial radiation decreases from 30.28 to 26.99 MJ m^{-2} during the period. Over the 15-day period, coefficients of variation in measured daily incoming longwave radiation (0.09) and outgoing longwave radiation (0.05) are low relative to variations in other radiation quantities. Day-to-day coefficients of variation (0.25) in net longwave radiation, calculated as the difference between these longwave radiation components, are high since the two components come close to a balance. The variation in net shortwave radiation (0.21) is about the same as the variation in both incoming and reflected shortwave radiation (0.21 and 0.22, respectively). Day-to-day variation in diffuse radiation totals are more extreme (0.42). On clear days diffuse radiation fluxes are small and change slowly during the day (see Fig. 4), but in variable weather conditions the diffuse radiation fluxes undergo large relative variations from day to day.

Intersite variability is substantially reduced on cloudy days relative to clear days. Reduction in variability comes from the lower levels of direct radiation (the primary factor causing differential insolation of sloping ecosystems), and an increase in diffuse radiation, which is more isotropic, providing a more general illumination of all ecosystems. The longwave terms also provide a moderating radiative influence. These effects were investigated by comparing PNL–RDG differences in daily radiation totals for 25 September to the PNL–RDG differences in average daily totals for a 7-day period of variable weather (16, 18, 20, 21, 22, 23 and 25 September) when equipment was functioning well. Intersite differences in net radiation during the variable weather period were only 0.46 of the clear day values. Similarly, values for $K\downarrow$, $K\uparrow$, $L\downarrow$, and $L\uparrow$ were 0.75, 0.58, 0.78, 0.56, and 0.18, respectively.

8. Summary and conclusions

Radiation budget measurements were made on the major topographic surfaces (i.e., valley floor, two sidewalls and a ridgetop) of Colorado's deep, semiarid Brush Creek Valley during a period near the autumnal equinox. The measurements were made to investigate the range of radiation and surface energy budget microclimates on the major surfaces within this single, well-defined, high altitude valley. Radiation budgets are described in the present paper; surface energy budgets are discussed in a companion paper (Whiteman et al. 1989). Since radiation instruments were installed only on the major topographic surfaces, we are unable to report on the full range of radiation microclimates in the valley. Nevertheless, a key finding is that daily and local sunrise to local sunset radiation budgets differ significantly on the major topographic surfaces. In fact, the site-to-site variation was larger than the standard deviation of day-to-day variations at a valley floor site during a 15-day period of unsettled weather in late September 1984.

A sagebrush ecosystem on the valley floor (site PNL) may be used to illustrate typical radiative fluxes in this climate setting. The sagebrush ecosystem at the time of the autumnal equinox during a clear day radiates a 24-h average of 371 W m^{-2} of longwave radiation, but receives longwave radiation at the rate of 283 W m^{-2}. The longwave deficit of 88 W m^{-2} is overcome during daytime by solar radiation. This radiation is received at the 24-h average rate of 230 W m^{-2}, of which 201 W m^{-2} is direct radiation and 29 W m^{-2} is diffuse radiation. Of the 230 W m^{-2} of solar radiation received, 33 W m^{-2} is reflected from the surface, leaving 197 W m^{-2} of net solar radiation. The radiation balance is therefore characterized by an excess of shortwave gain over the 24-h longwave loss, in the amount of 109 W m^{-2}. This net all-wave radiation excess must be balanced by nonradiative fluxes, including soil heat flux, latent heat flux and sensible heat flux.

It has been customary to summarize radiative fluxes at measurement sites in flat terrain by presenting daily and astronomical sunrise to astronomical sunset radiation totals. In complex terrain, it is often more appropriate to summarize radiation totals over the period from local sunrise to local sunset since several of the radiation variables change sign or undergo marked local oscillations in response to receipt of direct radiation. Comparison of local sunrise to local sunset totals between sites then includes the physically important effects of the differing periods of daylight at the sites due

to shading from surrounding terrain. This approach has been followed in the paper and has proven useful in differentiating site microclimates.

Radiative fluxes in the Brush Creek Valley are typical for radiation microclimates in which daytime solar radiation income is strong and directional. This results in important variations in incoming solar radiation on slopes of different aspect and inclination. This feature of the climate, supplemented by the propagation of shadows across the dissected terrain as the sun angles change through the day, causes important spatial and temporal variations in valley radiation fields. These variations can occur over small spatial scales when the terrain is finely dissected or when one site is in sunlight while another is in shade. This latter effect is quite strong on the southwest-facing sidewall in the afternoon and on the northeast-facing sidewall in the morning as the shadow of the opposite ridge propagates up or down the sidewall while the sun is still high in the sky. Differences in daily and daytime radiation totals at sites having identical surface orientations (e.g., horizontal sites on the ridgetop and valley floor) depend on the length of the daylight period, with sites deeper in the valley receiving a reduced period of daylight.

A special experiment was conducted to measure radiative fluxes over a steep sidewall on two sets of radiometers oriented horizontally and parallel to the underlying surface. Significant differences in measured radiation occurred in radiation streams having large directional (i.e., nonisotropic) components. Theoretical equations for translating the horizontal measurements to the underlying inclined surface worked reasonably well when simplifying assumptions were made, simulating both the variation in time and the daily totals. There are distinct operational advantages to orienting radiometers horizontally so that this result, if extended and bounded by observations in other climate settings, may prove useful to other investigators.

Mean daily radiation components were calculated for a 15-day period of variable weather at a valley floor site in late September 1984. The variable weather reduced the direct and net longwave radiation components and increased the diffuse radiation. The result was a general moderation of the microclimatic differences between sites and of the temporal extremes at a given site.

Acknowledgments. This research was supported by the U.S. Department of Energy under Contract DE-AC06-76RLO 1830 with Pacific Northwest Laboratory. Pacific Northwest Laboratory is operated by Battelle Memorial Institute for the U.S. Department of Energy.

REFERENCES

Brown, K. W., N. J. Rosenberg and P. C. Doraiswamy, 1970: Shading inverted pyranometers and measurements of radiation reflected from an alfalfa crop. *Water Resour. Res.*, **6**, 1782–1786.

Davies, J. A., P. J. Robinson and M. Nunez, 1970: Radiation measurements over Lake Ontario and the determination of emissivity. First Rep., Contract HO 81276, Department of Geography, McMasters University, Hamilton, Ontario.

Fritschen, L. J., and J. R. Simpson, 1989: Surface energy and radiation balance systems: general description and improvements. *J. Appl. Meteor.*, **28**, 680–689.

Miller, D. H., 1981: Energy at the surface of the earth. *International Geophysics Series,* Vol. 27, Academic Press, 516 pp.

Oke, T. R., 1978: *Boundary Layer Climates.* Methuen and Co. Ltd., 372 pp.

Steven, M. D., and M. H. Unsworth, 1979: The diffuse solar irradiance of slopes under cloudless skies. *Quart. J. Roy. Meteor. Soc.*, **105**, 593–602.

Whiteman, C. D., and K. J. Allwine, 1986: Extraterrestrial solar radiation on inclined surfaces. *Environmental Software,* **1**, 164–169.

——, R. Lambeth and K. J. Allwine, 1987: Major vegetation types, climatological data and solar radiation calculations for Colorado's Brush Creek Valley. PNL-6209/ASCOT-87-1, Pacific Northwest Laboratory, Richland, WA, 30 pp.

——, K. J. Allwine, M. M. Orgill, L. J. Fritschen and J. R. Simpson, 1989: Deep valley radiation and surface energy budget microclimates. Part II: Energy budget. *J. Appl. Meteor.*, **28**, 427–437.